

# LARGE AREA SCREEN PRINTED N-TYPE MC-SI SOLAR CELLS WITH B-EMITTER: EFFICIENCIES CLOSE TO 15% AND INNOVATIVE MODULE INTERCONNECTION

T. Buck<sup>1</sup>, R. Kopecek<sup>1</sup>, J. Libal<sup>1</sup>, R. Petres<sup>1</sup>, K. Peter<sup>1</sup>, I. Röver<sup>2</sup>, K. Wambach<sup>2</sup>, L.J. Geerligs<sup>3</sup>, E. Wefringhaus<sup>4</sup>, P. Fath<sup>4</sup>

<sup>1</sup> University of Konstanz, Faculty of Sciences, Department of Physics, D- 78457 Konstanz, Germany

<sup>2</sup> Deutsche Solar AG, Alfred-Lange Str. 18, D-09599 Freiberg/Sachsen, Germany

<sup>3</sup> Energy research Centre of the Netherlands – ECN, Westerduinweg 3, NL-1755 ZG Petten, The Netherlands

<sup>4</sup> now at: International Solar Energy Research Center Konstanz e.V., Rudolf Diesel Str. 15, D-78467 Konstanz, Germany

## ABSTRACT

In this paper we present n-type Si solar cells on large area mc-Si wafers with a boron diffused emitter at the front side. The focus of our studies is mainly related to the front surface of the solar cell. We have optimised  $BBr_3$ -diffusion and in-situ oxidation with respect to the homogeneity of the sheet resistance and substrate degradation. After diffusion even a slight improvement of the minority charge carrier lifetime was measured, which can be related to B-gettering. The emitter is contacted by AgAl-paste and passivated by thermal  $SiO_2$ . The development and optimisation of all processes led to solar cells with efficiencies of 14.7% on mc-Si and 17.1% on Cz-Si substrates.

In addition to this we present an innovative interconnection of modules using our developed cell (patent pending). We show an alternate serial interconnection of p- and n-type solar cells resulting in easier module processing.

## INTRODUCTION

There is a rising interest in n-type silicon for solar cell applications: besides being an additional feedstock source for the PV production it attracted attention by a higher tolerance to common impurities like Fe or O. The resulting higher diffusion lengths compared to p-type combined with reduced degradation due to the lack of B-O complexes qualifies the n-type material for high efficiency solar cells.

During the last years different, successful n-type solar cell concepts [1, 2] for industrial use have been reported but they concentrated on mono-crystalline Si material. In this paper we describe the development of industrial solar cells on n-type, directionally solidified mc-Si with a boron emitter based on techniques as open tube furnace diffusion and screen printing thick film metallization.

## EXPERIMENTAL

### Boron Diffusion

Because of its lower diffusivity boron has to be diffused longer or at higher temperatures than phosphorous to yield the same sheet resistance. Both possibilities mean a higher thermal budget which could be detrimental to mc-Si. Especially temperatures above  $1000^\circ\text{C}$ , as used commonly for Cz-Si devices are disadvantageous for the quality of mc-Si material.

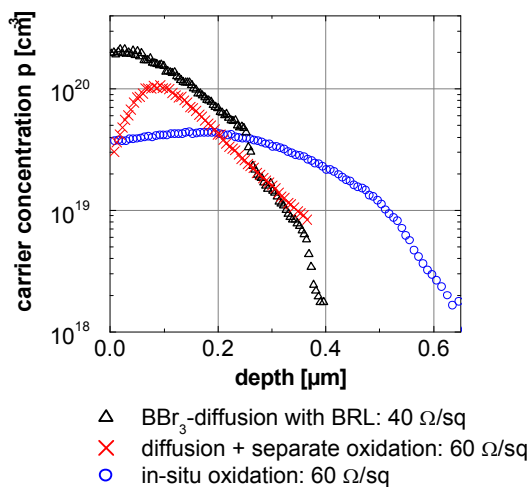


Fig.1. Diffusion profiles of B-emitters with and without BRL measured by ECV method.

To avoid this problem, our boron emitter diffusion was done at a moderate temperature of about  $900^\circ\text{C}$  with duration of 1h. Effective lifetime measurements of the bulk before and after the  $BBr_3$  open-tube furnace diffusion confirmed constant values averaged over the entire wafer and thus showed no degradation of the mc-Si.

Figure 1 shows the charge carrier concentration after different boron diffusions determined by Electrochemical Capacitance Voltage (ECV) measurement. The black triangles show the B-profile with so called "Boron Rich Layer" (BRL). This highly conductive layer occurs during the boron diffusion at the surface of the wafer and is resistant to chemical etching but can be removed by an oxidation step. As a consequence of the oxidation step the original sheet resistance of 40 Ohm/sq is increased to values of 60 Ohm/sq. If diffusion and oxidation are performed subsequently, the boron emitter becomes depleted at the surface of the wafer due to the higher solubility of boron in oxygen than in silicon as demonstrated in the red curve. To avoid this effect, diffusion and oxidation are combined in a so called in-situ oxidation process. As the boron glass remains on the wafer during the oxidation step the doping profile is less depleted as shown in the blue graph (circles). As the B-diffusion with in-situ oxidation is faster, easier and results in a more suitable emitter profile for contacting it was chosen for the emitter formation. Lifetime measurements on wafers before and after B-diffusion showed an improvement of the material quality [3] and suggest a gettering effect of the boron diffusion performed in clean ambient and at moderate temperature.

### Front surface passivation and metallisation

A good passivation of  $p^+$  Si surfaces is one of the key issues to be solved for a good performance of n-type solar cells with a B-emitter. If the emitter is on the front side this layer must in addition have good antireflective properties. Passivating experiments showed that  $\text{SiN}_x$  does not work on highly p-doped surfaces.

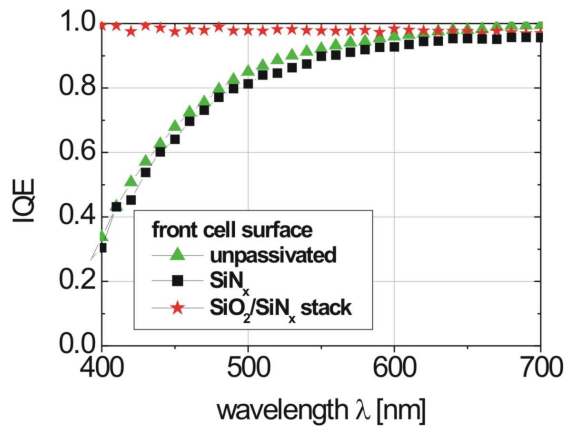


Fig. 2. IQE from spectral response measurements for different  $p^+$  front surface passivations of n-type solar cells.

As can be seen in Figure 2, the IQE analysis even reveals a slight depassivating behaviour of  $\text{SiN}_x$  compared to an unpassivated surface which was confirmed in systematic studies [3]. However,  $\text{SiO}_2$  is known for its excellent passivating properties on both  $p^+$  and  $n^+$ . If the oxide layer is thick enough, it even screens the "negative" effect of  $\text{SiN}_x$  and therefore offers the possibility of a  $\text{SiO}_2/\text{SiN}_x$  stack system. The stack additionally provides a good hy-

drogen passivation and can be adjusted in order to serve as an effective ARC. The red curve (cross) in Figure 2 documents the excellent internal quantum efficiency of the stack system and is even for wavelengths around 400 nm close to an optimum value of 1. Unfortunately the formation of a thermal oxide is an elaborate high temperature process that increases the thermal budget for the substrates and is hardly compatible to an industrial processing ambient.

The appliance of  $\text{SiC}_x$  as surface passivation could be a way to avoid these hindering accompaniments. It can be grown by a PECVD process comparable to  $\text{SiN}_x$  at low temperatures of about  $400^\circ\text{C}$  and is a one step process. Recent promising results by Petres et al. [4, 5] showed in QSSPC measurements implicit  $V_{oc}$  values for Cz material of 635 mV with this coating, which is comparable to results of  $\text{SiN}_x$  on  $n^+$  surfaces. Latest results will be presented at this conference [5].

The most suitable solution for the front side metallisation was the screen printing of commercial available Ag/Al paste. Despite its good contact resistance and print handling it suffers from a more than doubled line resistivity compared to standard Ag paste. Additional silver plating or double print of an Ag/Al and Ag stack reduced the series resistance. With future work in the field of grid optimisation and further metal paste testing a one step screen printing process with fill factors of 78% is feasible.

### SOLAR CELL STRUCTURE AND PROCESS

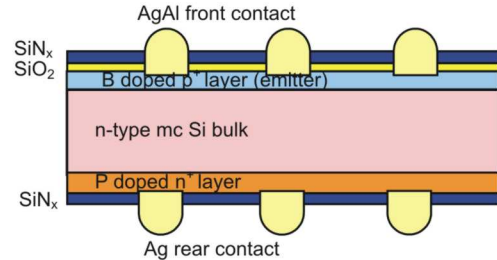


Fig. 3. Cross-section of the front B emitter n-type Si solar cell.

Figure 3 shows the formal structure of our device. The processing sequence shown in Fig. 4 is based on the process steps and processing techniques described above. The rear side is similar to the front side of a standard screen printed p-type Si solar cell, namely a  $50 \Omega/\text{sq}$  P-emitter contacted by Ag-paste and passivated by PECVD  $\text{SiN}_x$ . Solar cells have been made on both, large area Cz- and mc-Si substrates. The mc-Si substrates originate from directionally solidified ingots crystallized at Deutsche Solar and have a resistivity of about  $1 \Omega\text{cm}$  and an area of  $12.5 \times 12.5 \text{ cm}^2$ .

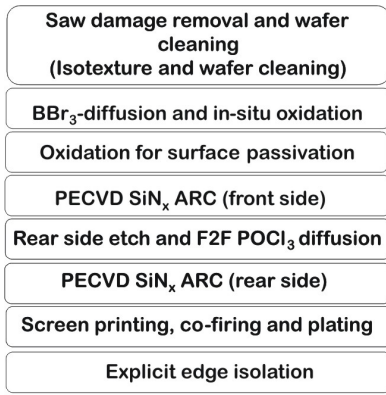


Fig. 4. Flowchart of solar cell process.

## RESULTS

The material shows a very good quality; the average bulk lifetime of the minority charge carriers is close to 200  $\mu\text{s}$  on as-grown 156  $\text{cm}^2$  wafers. Table 1 summarizes the best results obtained on Cz- and mc-Si material. Table 1a) shows the results for front side and 1b) for rear side illumination of these solar cells. The strong performance gap for this application derives from the different wafer thicknesses of the Cz (150  $\mu\text{m}$ ) and mc (230  $\mu\text{m}$ ) solar cells and the different effective diffusion lengths for these substrates both leading to a lower ratio of diffusion length to cell thickness ( $L_d/d$ ) for the mc solar cell. Especially the spectral response in the blue of the mc-Si solar cell suffers from the unfavourable ( $L_d/d$ ). On the other hand the monocrystalline cell is closer to an ideal value and therefore yields quantum efficiencies comparable to those of the front illumination as depicted in Figure 5.

### a) front illumination

| material | area [ $\text{cm}^2$ ] | res. [ $\cdot \text{cm}$ ] | FF [%] | $J_{sc}$ [ $\text{mA}/\text{cm}^2$ ] | $V_{oc}$ [mV] | $\eta$ [%] |
|----------|------------------------|----------------------------|--------|--------------------------------------|---------------|------------|
| Cz-Si    | 146                    | 2                          | 76     | 36.3                                 | 620           | 17.1       |
| mc-Si    | 144                    | 1                          | 74     | 32.8                                 | 602           | 14.7       |

### b) rear illumination

| material | d [ $\mu\text{m}$ ] | res. [ $\cdot \text{cm}$ ] | FF [%] | $J_{sc}$ [ $\text{mA}/\text{cm}^2$ ] | $V_{oc}$ [mV] | $\eta$ [%] |
|----------|---------------------|----------------------------|--------|--------------------------------------|---------------|------------|
| Cz-Si    | 150                 | 2                          | 74.9   | 29.5                                 | 610           | 13.5       |
| mc-Si    | 230                 | 1                          | 74.8   | 16.6                                 | 580           | 7.2        |

Table 1a). Parameters of best solar cells obtained by the process described in Figure 3. 1b). Parameters of the same solar cells for rear illumination.

## Bifacial character of solar cells

As described above, the processing scheme features a transparent rear side with an open rear contact of the solar cells. As a consequence, light injection is possible from both, front and rear side of the device. For applications on reflective surface like sand or water a remarkable ratio of scattered light can be captured from the rear side and so increase the power output of the solar cell [6].

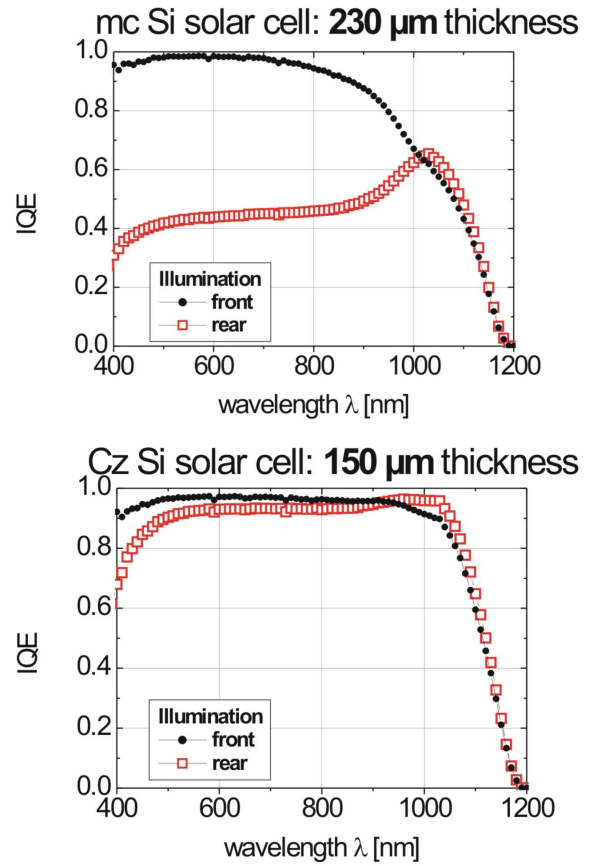


Fig. 5. IQE from spectral response measurements of best mc- and Cz-Si solar cell for front and rear side illumination.

Especially the use of thin substrates combined with high diffusion lengths of the material can lead to a significant increase of the power if there is additional radiation from the rear side. Fig. 6 shows a PC1D simulation based on the Cz-Si solar cell results to illustrate the relation between cell thickness, rear illumination and corresponding power increase.

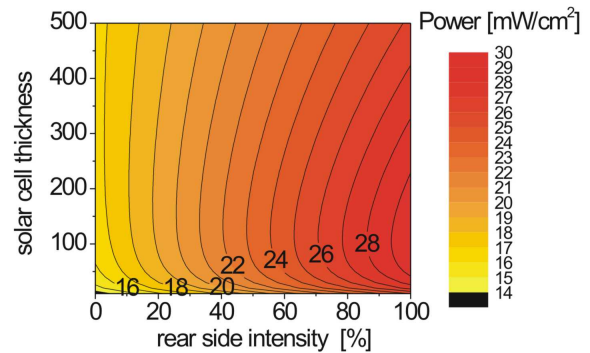


Fig. 6. Simulated power output for a bifacial solar cell as a function of cell thickness and additional illumination intensity from rear

For a rear side intensity that matches 20% of the front side radiation, estimated 18% additional power can be supposed for a 200  $\mu\text{m}$  solar cell. Recent experiments with a p-type bifacial test module confirmed the order of magnitude as a realistic estimation. The results are summarized by Kränzl et al. [6] in an additional paper in these proceedings.

### Cell interconnection in module

Another essential advantage and technological innovation connected to our developed  $\text{p}^+\text{nn}^+$ -type solar cells is that they can be used for module fabrication together with standard industrial screen-printed  $\text{n}^+\text{pp}^+$ -type solar cells allowing a simplification in the stringing process as well as the increase in module efficiency. Conventional interconnection of screen printed p-type solar cells always links the front side with the rear side of a neighbouring wafer (Fig. 7a).

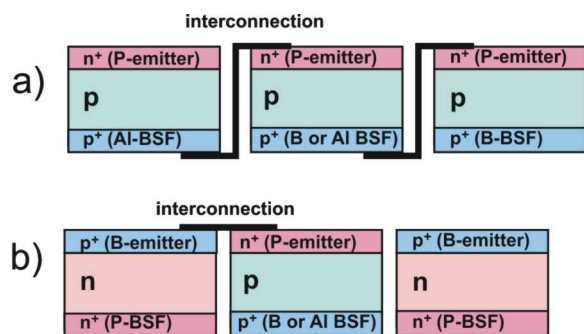


Fig. 7. a) Conventional module interconnection: each cell backside is connected with the front side of the subsequent solar cell. b) Innovative interconnection using alternating p-type and n-type solar cells.

This procedure demands to flip the solar cells during the tabbing process which is a delicate and time consuming work. If p- and n-type solar cells, on the other hand, are alternatingly stringed in one frame such as depicted in Figure 7b) the flipping is not necessary any more. Additionally, the solar cells can be packed closer together in the module and new possibilities like combining the metalization with module gluing are supposable (patent pending).

To demonstrate the successful operation of the concept, two double side glass modules were processed at SOLTECH, Belgium – one with six 157  $\text{cm}^2$  standard screen printed p-type mc-Si and one with 144  $\text{cm}^2$  bifacial alternately interconnected three p- and three n-type cm-Si solar cells. The modules were measured with a flash tester in a dark area with no reflection on the rear side of the module (see Tab. 2). The  $V_{oc}$  for the standard module is 3.7 V compared to 3.6 V for the pn-type module and the  $I_{sc}$  4.7 A (cell: 29.9  $\text{mA}/\text{cm}^2$ ) for the standard compared to 4.5 A (cell: 31.3  $\text{mA}/\text{cm}^2$ ) for the pn-type module. The fill factor in the case of the standard module is 77% while that of the pn-type module is only 72% because of the overall

lower fill factor of the bifacial solar cells so far. As this is merely due to the high series resistance of the open rear contact the fill factor can be easily increased by the optimisation of the rear grid design.

| type          | standard module | pn-type module |      |
|---------------|-----------------|----------------|------|
|               |                 | front          | rear |
| illumination  | front           | front          | rear |
| $V_{oc}$ [V]  | 3.7             | 3.6            | 3.5  |
| $I_{sc}$ [A]  | 4.7             | 4.5            | 2.6  |
| $V_{mpp}$ [V] | 3.0             | 2.8            | 3.0  |
| $I_{mpp}$ [A] | 4.5             | 4.2            | 2.3  |
| $P_{mpp}$ [W] | 13.4            | 11.7           | 6.7  |
| FF [%]        | 77.1            | 71.5           | 73.4 |

Table 2. Module parameters for the standard and pn-type module from flash tests.

### SUMMARY

We have presented a low cost solar cell process for n-type mc-Si wafers which has resulted in an efficiency of 14.7% for a cell area of 154  $\text{cm}^2$ . Devices on Cz-Si material exceeded an efficiency of 17%. The bifacial geometry allows applications for a simultaneous two sided illumination and showed an increase of power up to 20%. It was demonstrated that the introduced cell structure with a front boron emitter is advantageous for module fabrication if combined with standard p-type solar cells. It allows an innovative, simplified cell interconnection. A first demonstration module of this new type was fabricated and showed a good performance.

### ACKNOWLEDGEMENTS

This work was supported by funding of the German BMU under contract number 0329844F (OPTIMAN) and is continued in the European FoXy Project (019811-SES6-FOXY).

### REFERENCES

- [1] M. Taguchi et al., "An approach for the higher efficiency in the HIT Cells", *Proc. 31<sup>st</sup>. IEEE PVSC*, (2005)
- [2] W.P. Mulligan et al., "manufacture of solar cells with 21% efficiency", *Proc. 19<sup>th</sup> EPVSEC*, (2004), pp 387
- [3] J. Libal et al., "n-type multicrystalline silicon solar cells,  $\text{BBr}_3$  diffusion and passivation of  $\text{p}^+$  diffused silicon surfaces", *20<sup>th</sup> EPSEC*, 2005, pp. 793-796
- [4] R. Petres et al., "Passivation of surfaces by PECVD silicon carbide films" *Proc. 15<sup>th</sup> PVSEC*, 2005, pp. 128-129
- [5] R. Petres et al., "Improvements in the low-temperature passivation of  $\text{p}^+$  Si surfaces by PECVD silicon carbide films", *these proceedings*
- [6] A. Kränzl et al., "Bifacial solar cells on multi-crystalline silicon with boron BSF and open rear contact", *these proceedings*